

Controlled Photoredox Ring-Opening Polymerization of O-Carboxyanhydrides

Quanyou Feng^{†,‡} and Rong Tong^{*,‡}

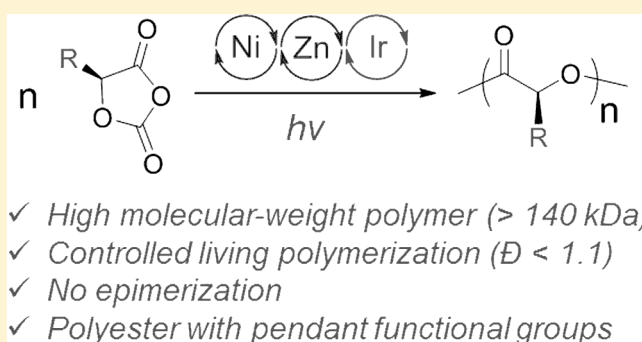
[†]Center for Molecular Systems and Organic Devices, Institute of Optoelectronic Materials, Key Laboratory for Organic Electronics and Information Displays & Institute of Advanced Materials, Jiangsu National Synergetic Innovation Center for Advanced Materials, Nanjing University of Posts and Telecommunications, 9 Wenyuan Road, Nanjing 210023, China

[‡]Department of Chemical Engineering, Virginia Polytechnic Institute and State University, 635 Prices Fork Road, Blacksburg, Virginia 24061, United States

S Supporting Information

ABSTRACT: Poly(α -hydroxy acids) are important biodegradable polymers with wide applications. Attempts to synthesize them from O-carboxyanhydrides with pendant functional groups by various methods, including methods involving organocatalysts or organometallics, have been plagued by uncontrolled polymerization, including epimerization for some monomers, which hampers the preparation of stereoregular high-molecular-weight polymers. Herein we describe an effective protocol that combines photoredox Ni/Ir catalysis with the use of a Zn-alkoxide for efficient ring-opening polymerization, allowing for the synthesis of isotactic polyesters with expected molecular weights (>140 kDa) and narrow molecular weight distributions ($M_w/M_n < 1.1$).

Mechanistic studies indicate that the use of a low temperature ($-20\text{ }^\circ\text{C}$) and photoredox Ni/Ir catalysis synergistically accelerates ring-opening and decarboxylation of the monomer for chain propagation while avoiding the formation of the undesired Ni-carbonyl complex.



INTRODUCTION

Poly(α -hydroxy acids) (PAHAs), including polylactide, are widely used in everyday applications ranging from clothing and packaging to agriculture and biomedicine.¹ However, their utility for applications that demand physicochemical properties such as stiffness, ductility, and tensile strength is greatly limited by the lack of side-chain functionality in PAHAs and in their monomers (lactones),² which are usually synthesized by multistep methods that are difficult to scale up.³ Since 2006, O-carboxyanhydrides (OCAs), which can be prepared with a rich variety of side-chain functionalities,⁴ have emerged as an alternative class of highly active monomers for polyester polymerization (Figure 1a).^{4a,5} Unfortunately, current synthetic methods, especially those involving organocatalysts, result in uncontrolled polymerization including epimerization (i.e., lack of stereoregularity) for OCAs bearing electron-withdrawing groups,^{4c,6} unpredictable molecular weights (MWs), or slow polymerization kinetics (Table S1).^{5a,7} Recently, we reported an active organometallic complex, (BDI-IE)Zn-OCH(Me)COOMe (BDI-IE = 2-((2,6-diethylphenyl)amino)-4-((2,6-diisopropylphenyl)imino)-2-pentene), that catalyzes well-controlled ring-opening polymerization (ROP) of OCAs at a low degree of polymerization ($DP \leq 200$) without epimerization (Figure 1b).⁷ However, this Zn-alkoxide catalyst cannot efficiently produce polymers with a high degree of polymerization ($DP \geq 300$, Table S1). Because of the above-

described limitations, the development of a viable catalyst that can mediate controlled polymerization to prepare stereoregular, high-MW PAHAs is crucial.

Visible-light photoredox catalysis has recently emerged as a powerful technique for radical polymerization⁸ and organic synthesis.⁹ Photoredox catalysts and nickel catalysts reportedly can be successfully combined for the decarboxylation of carboxylic acids and anhydrides via a catalytic cycle involving single-electron transfer (Figure 1c).¹⁰ Nickel catalysts also mediate the ROP of N-carboxyanhydrides, structural analogues of OCAs (Figure 1c).¹¹ Historically, nickel catalysts have been used to mediate the cross-coupling of redox-active carboxylic acids¹² or anhydrides¹³ with organozinc agents (Figure 1c). On the basis of these previously reported results, we hypothesized that a Ni/photoredox catalyst system to accomplish OCA decarboxylation could be merged with a Zn catalyst to mediate ring opening of OCAs in a manner similar to that observed for anhydrides,^{10b} generating an active Zn-alkoxide chain end for chain propagation and thus enabling controlled synthesis of high-MW polymers (Figure 1d).

Received: February 10, 2017

Published: April 11, 2017

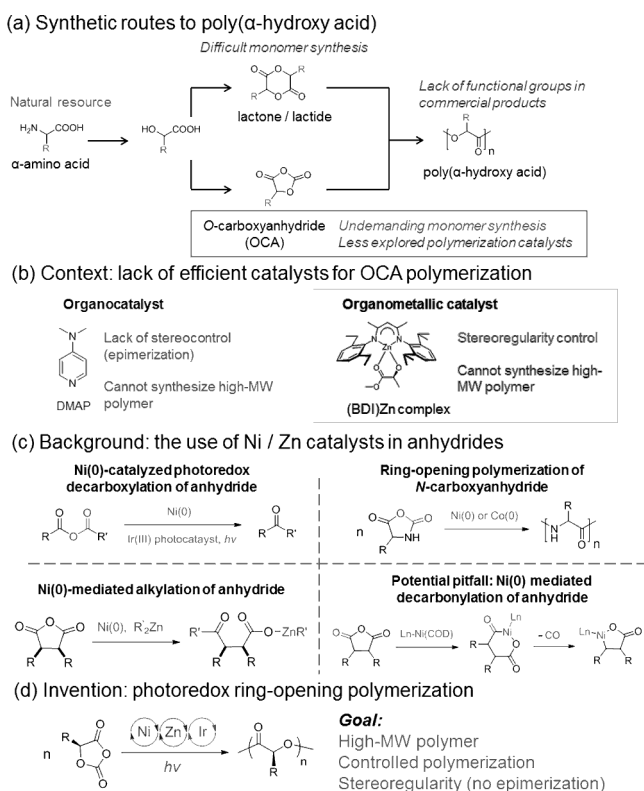


Figure 1. Photoredox ring-opening polymerization of *O*-carboxyanhydrides (OCAs). (a) Synthetic routes to poly(α -hydroxy acid). (b) Previously reported catalysts for ring-opening polymerization of OCAs. (c) Reported uses of Ni/Zn cocatalysts for reactions of anhydrides, and Ni-mediated decarbonylation as a potential side reaction. (d) Photoredox ring-opening polymerization reported in this paper.

RESULTS AND DISCUSSION

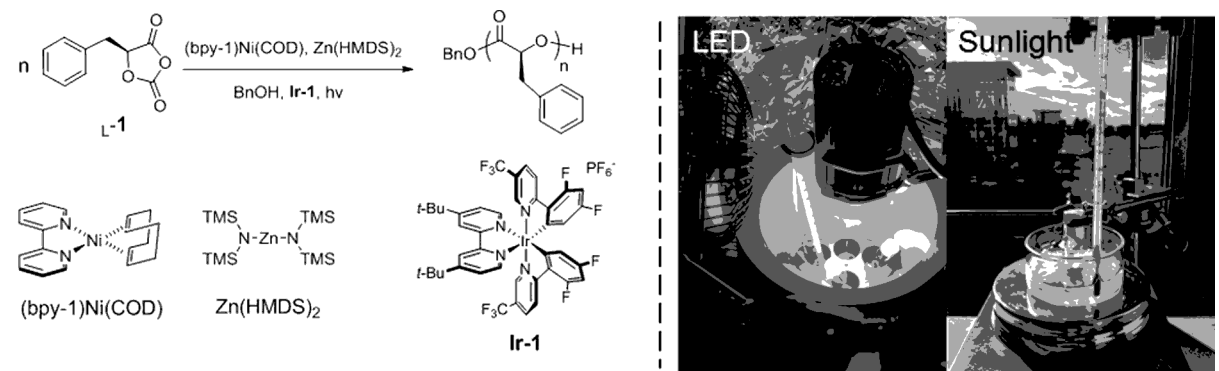
Optimization of Photoredox Polymerization Conditions. With this hypothesis in mind, we began by investigating the ROP of *L*-Phe-OCA (**L-1**, Table 1), which was readily prepared in two steps from commercially available *L*-phenylalanine on a multigram scale.^{4f} We discovered that within 4 h at room temperature, the combination of (bpy-1)Ni(COD) (bpy-1 = 2,2'-bipyridyl, COD = 1,5-cyclooctadiene), Zn(HMDS)₂ (HMDS = hexamethyldisilazane), and Ir[dF(CF₃)ppy]₂(dtbbpy)PF₆ (**Ir-1**, dF(CF₃)ppy = 2-(2,4-difluorophenyl)-5-(trifluoromethyl)pyridine, dtbbpy = 4,4'-di-*tert*-butyl-2,2'-bipyridine) in the presence of blue LEDs (400–500 nm) and benzyl alcohol (BnOH) as the initiator resulted in complete monomer consumption and generation of a product with a number-average MW (M_n) of 39.2 kDa and a MW distribution ($\mathcal{D} = M_w/M_n$) of 1.10 ($[L-1]/[Ni]/[Zn]/[BnOH]/[Ir-1] = 300/1/1/1/0.1$; entry 1). However, at a higher monomer feed ratio ($[L-1]/[Ni]/[Zn]/[BnOH]/[Ir-1] = 500/1/1/1/0.1$), uncontrolled polymerization occurred, affording a polymer with a M_n of 38.1 kDa and a broad \mathcal{D} of 1.71 (entry 2).

Surprisingly, optimization of other reaction parameters revealed that excellent polymerization control was achieved by carrying out the reaction in a cooling bath at -15 °C for 6 h (Table 1, entry 3); these conditions afforded a polymer with a M_n of 78.4 kDa, which is close to the expected MW (74.1 kDa), and a narrow \mathcal{D} of 1.05. During the polymerization, the reaction solution turned from orange to light purple, suggesting regeneration of a Ni(0) complex; (bpy-1)Ni(COD) is a deep purple color (Figure S1). Under these low-temperature

conditions, M_n of the poly(**L-1**) product increased linearly with initial $[L-1]/[Ni]/[Zn]/[Ir-1]$ ratio up to 1000/1/1/0.1, and all of the \mathcal{D} values were <1.1 (Figure 2a,b), which indicates that chain-breaking reactions did not occur during the ROP.¹⁴ Notably, even for high-MW poly(**L-1**) (entry 4, $M_n = 140.5$ kDa), no epimerization of the α -methine hydrogen was observed in the homodecoupling ¹H NMR spectrum (Figure 2c), indicating that the Ni and Zn complexes did not affect OCA chirality during the ROP.

We demonstrated the necessity of each of the catalytic components by means of a series of control experiments (Table 1, compare entry 5 with entries 6–11; Table S2). At a high DP of 500, neither (bpy-1)Ni(COD) alone (Table S2, entry 3) nor Zn(HMDS)₂ combined with BnOH (entry 4) was able to initiate polymerization. Without the Ni complex the polymerization was uncontrolled, whereas the Zn complex was essential for chain propagation (Table 1, entries 6 and 7, respectively). Either (bpy-1)Ni(COD) or Zn(HMDS)₂ could initiate polymerization but in an uncontrolled manner with incomplete monomer conversion (Table S2, entries 3 and 5). When the reaction was carried out without BnOH, the obtained polymer had uncontrolled M_n and \mathcal{D} values (entry 8). Additionally, electrospray ionization mass spectrometry (ESI-MS) analysis of oligo(**1**) at a DP of 5 confirmed the attachment of the BnO group to the oligomer (Figure 2d; high-resolution ESI-MS results in Figure S2), suggesting that a Zn-alkoxide was involved in ring-opening and chain propagation. Additionally, oligo(**1**) without the attachment of BnO group was not observed in the ESI-MS spectrum. To verify the incorporation of the alcohol initiator in the polymerization, 1-pyrenebutanol was used to initiate photoredox oligomerization of **1** (DP = 15). The incorporation efficiency was over 95% as determined by HPLC (Figure S4), confirming the necessity of Zn-alkoxide for efficient initiation. Moreover, either incomplete monomer conversion or uncontrolled polymerization occurred in the absence of Ir-1 (entry 9), light (entry 10), or both (Table S2, entries 8 and 9). We also found that monomer conversion was only 39% when TEMPO, a radical-trapping agent,¹⁵ was present in the reaction mixture (Table S2, entry 10), indicating the indispensability of photoinduced electron transfer in this photoredox polymerization. Finally, when LED light was replaced with sunlight, the reaction still proceeded smoothly to completion within 4 h (Table 1, entry 11).

Effects of Ni and Zn Complex Ligands on the Polymerization. During the optimization process, we also investigated the effects of the Ni and Zn ligands (Tables S3 and S4). We found that the substituents on the bpy ligand of the Ni complex did not markedly affect the polymerization results (Table S3, entries 1–3) and that bpy, phenanthroline, and PCy₃ (PCy₃ = tricyclohexylphosphine) were better ligands than PPh₃ (PPh₃ = triphenylphosphine) (entries 1 and 4–6) for the polymerization without irradiation at room temperature; a Ni(0) complex with a PPh₃ ligand gave a polymer with an extremely high M_n (entry 5). The weaker Ni-PPh₃ bond strength, compared to that of very basic PCy₃ ligand,¹⁶ may affect the polymerization results. The use of Ni(II) complexes failed to afford polymers (entries 7 and 8). We tested ligands that worked at room temperature in the photoredox polymerization at -15 °C. The use of Ni complexes with bpy-2 or phenanthroline ligands results in much higher MW than expected (entries 9–10). We also found that sterically bulky BDI-Zn complexes did not initiate controlled polymerization at a DP of 300 (Table S4, entries 1–10), even using photoredox ROP conditions (entry

Table 1. Optimization of Conditions for Ring-Opening Polymerization of L-1^a


entry	conditions	DP ^b	temp. (°C)	time (h)	conv. (%) ^c	M _n (kDa) ^d	MW _{cal} (kDa)	Đ ^d
1	as shown	300	r.t.	4	100	39.2	44.5	1.10
2	as shown	500	r.t.	4	100	38.1	74.1	1.71
3	as shown	500	-15	6	100	78.4	74.1	1.05
4	as shown	1000	-15	8	100	140.5	148.1	1.05
5	as shown	300	-15	4	100	47.2	44.5	1.01
6	no (bpy-1)Ni(COD)	300	-15	4	100	101.8	44.5	1.39
7	no Zn(HMDS) ₂	300	-15	4	20	4.8	44.5	4.61
8	no BnOH	300	-15	4	97	62.9	44.5	1.73
9	no Ir-1	300	-15	4	100	54.8	44.5	1.45
10	no light	300	-15	4	100	48.9	44.5	1.30
11	sunlight instead of LED	300	-15	4	100	54.6	44.5	1.06

^aAbbreviations: DP, degree of polymerization; Temp., temperature; Conv., monomer conversion; M_n, number-average molecular weight; MW_{cal}, molecular weight calculated on the basis of the ratio of the amount of monomer to the amount of the catalyst; Đ, molecular weight distribution; r.t., room temperature. ^bDP refers to the ratio of the amount of monomer to the amount of the catalyst. ^cDetermined from the intensity of the Fourier transform infrared peak at 1805 cm⁻¹, which corresponds to the OCA anhydride group. ^dDetermined by gel-permeation chromatography.

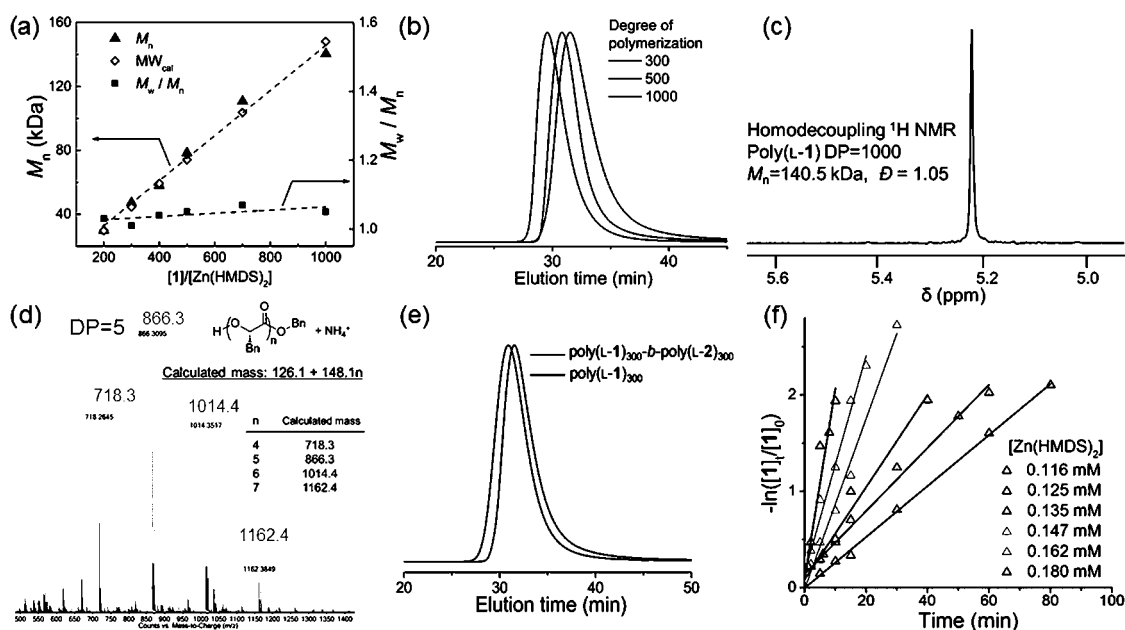
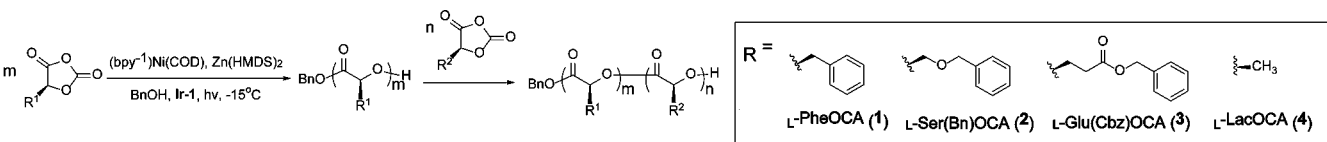


Figure 2. Controlled photoredox ring-opening polymerization of OCAs. (a) Plots of M_n and molecular weight distribution (M_w/M_n) of poly(L-1) versus $[L-1]/[Zn(HMDS)_2]$ ratio ($[(bpy-1)Ni(COD)]/[Zn(HMDS)_2]/[BnOH]/[Ir-1] = 1/1/1/0.1$). (b) Representative gel-permeation chromatography (GPC) traces of the photoredox polymerization reaction in panel (a). (c) Homodecoupling ¹H NMR spectrum of the α -methine region of poly(L-1) with a degree of polymerization (DP) of 1000. (d) Electrospray ionization mass spectrum (ESI-MS) of oligo(L-1)₅ formed by BnOH-initiated polymerization (high-resolution ESI-MS results in Figure S2). (e) Representative GPC traces of poly(L-1)₃₀₀ and the block copolymer poly(L-1)₃₀₀-b-poly(L-2)₃₀₀ (Table 2, entry 4). (f) Plots of L-1 conversion versus time at various Zn(HMDS)₂ concentrations, showing first-order kinetics. $[L-1] = 81.1$ mM; $[(bpy-1)Ni(COD)]/[Zn(HMDS)_2]/[BnOH]/[Ir-1] = 1/1/1/0.1$.

13), whereas a less bulky tridentate ligand did (entries 11 and 12).¹⁷

Homopolymerization and Copolymerization of Various OCAs. To evaluate the generality of our photoredox Ni/Zn

Table 2. Photoredox Polymerization and Block Copolymerization of Various OCA Monomers.^a


entry	monomer	DP ^b	time (h)	conv. (%) ^c	M _n (M _n -b1) (kDa) ^d	MW _{cal} (MW _{cal} -b1) (kDa) ^d	Đ (Đ-b1) ^d
1	2	400	8	100	65.7	71.3	1.05
2	3	300	5	100	72.7	66.1	1.04
3	4	300	6	100	24.1	21.7	1.04
4	1/2	300/300	4/12	100	112.7 (50.6)	97.9 (44.5)	1.04 (1.05)
5	2/1	100/200	3/4	100	63.2 (21.5)	47.5 (17.9)	1.07 (1.05)
6	1/3	200/100	3/3	100	46.7 (25.6)	51.7 (29.7)	1.06 (1.06)
7	3/1	300/200	5/4	100	86.2 (72.7)	95.7 (66.1)	1.06 (1.04)
8	1/4	200/100	4/3	100	37.6 (29.9)	36.9 (29.7)	1.05 (1.06)
9	2/3	100/100	4/3	100	46.7 (25.6)	39.9 (17.9)	1.02 (1.02)
10	3/2	300/100	5/3	100	89.7 (72.7)	83.9 (66.1)	1.05 (1.04)
11	2/3/1	100/100/100	3/3/3	100	66.2 (18.0)	54.7 (17.9)	1.04 (1.02)

^aAbbreviations: DP, degree of polymerization; temp., temperature; conv., monomer conversion; M_n, number-average molecular weight; MW_{cal}, molecular weight calculated on the basis of the amount of monomer to the amount of the catalyst; Đ, molecular weight distribution. M_n-b1 and Đ-b1 refer to the molecular weight and molecular weight distribution of the first block polymer. ^bDP refers to the ratio of the amount of monomer to the amount of the catalyst. ^cDetermined from the intensity of the Fourier transform infrared peak at 1805 cm⁻¹, which corresponds to the OCA anhydride group. ^dFor homopolymers, M_n and Đ were determined by gel-permeation chromatography (GPC). For copolymers, M_n-b1, Đ, and Đ-b1 were determined by GPC; M_n of the block copolymer was calculated on the basis of the ¹H NMR integration ratio of the α-methine peaks of the different blocks.

catalytic system, we carried out ROP reactions of three other OCA monomers (2–4; Table 2, entries 1–3). In all cases, polymers were obtained with excellent polymerization control, similar to that for poly(L-1). All the M_n values were close to the calculated MWs, and the Đ values were <1.1. Epimerization at the α-methine hydrogen did not occur (Figures S5–S7). Diblock and triblock copolymers could also be readily prepared in one pot by sequential addition of the monomers, and remarkable control of the M_n and Đ values was achieved (entries 4–11; Figure 2e). We also found the random photoredox copolymerization of 1 and 3 (200/200) resulted in complete monomer conversion and generation of a random-sequenced copolymer with a M_n of 76.8 kDa and a Đ of 1.05, close to the expected MW (73.7 kDa, Figure S8).

Kinetics. We then examined the kinetics of the photoredox ROP of L-1 by varying the concentration of each reaction component and monitoring the monomer conversion by Fourier transform infrared (FTIR) spectroscopy.^{7,18} The reaction was first-order with respect to L-1 (Figure 2f) and zero-order with respect to BnOH and Ir-1, whereas the reaction orders with respect to (bpy-1)Ni(COD) and Zn(HMDS)₂ were 1.84 ± 0.26 and 2.49 ± 0.27, respectively (Figure S9). These results indicate that the rate of chain propagation was independent of both BnOH and Ir-1. The propagation rate independence of BnOH indicates that BnOH was only involved in the initiation but not chain propagation. Similarly, Ir-1 possessing a long-lived excited state likely only influenced the Ni complex oxidation state via single electron transfer cycle,¹⁰ without affecting the chain end reactivity. The fractional reaction orders for the Ni and Zn complexes were presumably due to the formation of separate aggregates of each complex, which was also observed in the ROP of lactide by Zn or Al complexes.^{18,19} To explore whether Ni and Zn catalysts formed a coordinate complex to mediate the polymerization, we fixed the Ni/Zn ratio at 1/1 in the kinetic study and found the reaction order was 4.66 ± 0.26 (Figure S9b). This value is close to the sum of the individual reaction order of

Zn(HMDS)₂ (2.49 ± 0.27 in Figure S9d) and (bpy-1)Ni (1.84 ± 0.26 in Figure S9f), suggesting no formation of Ni–Zn complex during the polymerization (confirmed by the NMR studies in Figure S10). These experiments suggest that the kinetics of the photoredox ROP of L-1 can be described by the following equation:

$$-d[L-1]/dt = k_p [Ni]^{1.84} [Zn]^{2.49} [L-1]^1 \quad (1)$$

where k_p is the rate constant for chain propagation.

Mechanistic Studies. The success of the photoredox Ni/Zn catalytic system prompted us to explore the mechanism of the reaction. The ring-opening reaction of 1 was examined by means of low-temperature NMR analysis of a mixture of (PCy₃)₂Ni(COD), Zn(HMDS)₂, BnOH, and 1 (1 equiv of each) with Ir-1 (0.1 equiv) under irradiation with light at –20 °C; we used the PCy₃ ligand so that we could elucidate the intermediate Ni complexes. No (PCy₃)₂Ni(CO) or (PCy₃)₂Ni(CO)₂ was observed in the ³¹P NMR spectrum (Figure 3a(i)). Both the ¹³C NMR results (the disappearance of the carbonyl peak at 149 ppm, Figure 3b(i)) and the FTIR results (the shift in ν(CO) from 1810 to 1750 cm⁻¹; Figure S11(a5)) confirmed the complete ring-opening of 1.

In contrast, Ni-carbonyl complexes were observed in the ³¹P NMR spectrum of the same mixture at room temperature ((PCy₃)₂Ni(CO) at 37.9 ppm, (PCy₃)₂Ni(CO)₂ at 41.0 ppm; Figure 3a(iv)),²⁰ which was also confirmed by the ¹³C NMR spectrum (Figure 3b(iii)),²¹ suggesting the formation of a nickelacycle intermediate by means of an oxidative addition reaction between Ni(0) and 1 at room temperature (Figure 3a, reaction scheme).^{11b,22} In addition, oxidative addition of a Ni(0) complex to 1 likely occurred regioselectively at the O₁–C₅ bond of 1, similar to the case for N-carboxyanhydride.¹¹ This possibility was supported by the absence of an anhydride stretching vibration (1820–1800 cm⁻¹) in the FTIR spectrum of 1/(PCy₃)₂Ni(COD) (Figure S8(a1)) and by the appearance of a carbonate peak (160 ppm) in the ¹³C NMR spectrum of the 1/

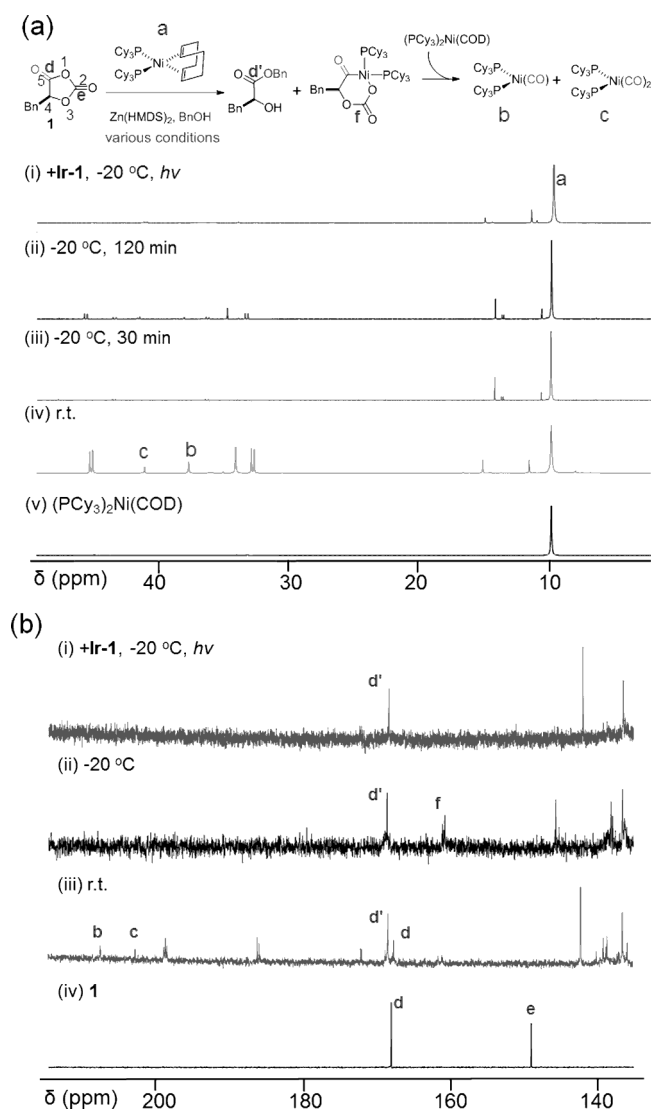


Figure 3. Mechanistic studies of the photoredox ring-opening reaction of L-1. (a) ^{31}P NMR and (b) ^{13}C NMR spectra obtained under various reaction conditions. $[\text{L-1}]/[(\text{PCy}_3)_2\text{Ni}(\text{COD})]/[\text{Zn}(\text{HMDS})_2]/[\text{BnOH}]/[\text{Ir-1}] = 1/1/1/0.1$. The gray area in (a) indicates the side products.

$(\text{PCy}_3)_2\text{Ni}(\text{COD})/\text{Zn}(\text{HMDS})_2/\text{BnOH}$ mixture (Figure 3b–b(iii)). We also explored the nickelacycle formed from $(\text{PCy}_3)_2\text{Ni}(\text{COD})$ and **1**.^{11,22d} From the mixture of $(\text{PCy}_3)_2\text{Ni}(\text{COD})$ and **1**, a hexane-soluble red oil and a THF-soluble yellow powder were isolated (Figure S12). The ^{31}P NMR (same as in Figure 3a) and FTIR analysis of the oil ($\nu(\text{Ni}(\text{CO})) = 1979$ and 1940 cm^{-1}) confirmed the presence of $(\text{PCy}_3)_2\text{Ni}(\text{CO})$ and $(\text{PCy}_3)_2\text{Ni}(\text{CO})_2$ (Figure S12b,d). The nickel–OCA complex could not be recrystallized or isolated from the hexane solution, but the doublet set in ^{31}P NMR suggested its presence (Figure S12b).^{22d} The hexane-insoluble powder was presumably oligo(**1**), as indicated by ^{13}C NMR (only 168 ppm peak and no other peaks above 140 ppm, Figure S12c) and FTIR analysis ($\nu(\text{COO}) = 1758\text{ cm}^{-1}$, Figure S12e). The uncontrolled polymerization of **1** by $(\text{bpy-1})\text{Ni}(\text{COD})$ was also observed (Table S2, entry 3), suggesting that oligo(**1**) was formed via the undesired Ni-mediated ring-opening reaction. In addition, the use of low temperature but no light could not avoid the Ni-mediated carbonylation over the time (Figure 3a, (ii) versus (iii)).

Notably, both the ^{13}C NMR results ($\text{C}_5(\text{O})$ at 178 ppm, slight shift of C_2 from 147 to 152 ppm; Figure S13b) and the FTIR results ($\nu(\text{Zn}(\text{CO})) = 1948\text{ cm}^{-1}$,²³ Figure S11(a2)) indicate that the Zn-alkoxide complex likely inserted into the $\text{O}_1\text{--C}_5$ bond, in a way similar to that in the Ni(0) complex. However, the insertion of Zn-alkoxide into **1** was not followed by efficient decarboxylation, indicated by the presence of both $\text{C}_2(\text{O})$'s monomer peak and carbonate peak (147 and 152 ppm, Figure S13b). Comparison of the results obtained using Zn-alkoxide with those obtained with the Ni/Zn dual catalyst (the ^{13}C NMR spectrum showed an ester peak at 167 ppm but no $\text{C}_5(\text{O})$ peak at 178 ppm and no $\text{C}_2(\text{O})$ peaks from 155 to 145 ppm; Figure 3b(i–iii)) indicates that a Ni complex likely added oxidatively to **1** before coordination and insertion of the Zn-alkoxide.

To confirm that a Ni-mediated decarbonylation side reaction did not occur in the low-temperature photoredox ring-opening reaction, we carried out the ring-opening reaction with Wilkinson's catalyst, $(\text{PPh}_3)_3\text{RhCl}$, an extremely effective CO scavenger (Figure S11).²⁴ Both at room temperature and at $-15\text{ }^\circ\text{C}$ (1 equiv of **1**, $(\text{bpy-1})\text{Ni}(\text{COD})$, $\text{Zn}(\text{HMDS})_2$, BnOH , and $(\text{PPh}_3)_3\text{RhCl}$), the carbonyl stretching vibrations (1976 and 1917 cm^{-1}) of $(\text{PPh}_3)_2\text{Rh}(\text{CO})\text{Cl}$ were observed in the FTIR spectrum of the reaction mixture (Figure S11(b3),(b4)), but they were not present in the reaction mixture containing the photoredox catalyst Ir-1 (0.1 equiv) under irradiation at $-15\text{ }^\circ\text{C}$ (Figure S11(b5)), confirming that only decarboxylation occurred in this system. Because both decarbonylation and decarboxylation reportedly occur during the oxidative addition of Ni(0) complexes to anhydrides (Figure 1c),²⁵ our results clearly indicate that irradiation under low-temperature conditions in the presence of photoredox catalyst Ir-1 accelerated decarboxylation while avoiding the formation of a Ni-carbonyl, which is detrimental to the ROP.¹⁰ Note that no reaction was observed when $\text{Zn}(\text{HMDS})_2$ and $(\text{bpy-1})\text{Ni}(\text{COD})$ were present at a 1/1 ratio (Figure S10) ruling out the formation of a Zn–Ni coordination complex prior to the ROP.²⁶

On the basis of our results and by analogy to prior mechanistic investigations of Ni-catalyzed coupling reactions of anhydrides and alkylzinc agents,²⁶ we propose the following catalytic pathway (Figure 4). First, oxidative addition of a Ni(0) complex to **1** leads to a nickelacycle intermediate, which undergoes photoinduced decarboxylation and transmetalation with a Zn complex to generate a reactive Zn-alkoxide terminus for chain propagation. Of note, Ni-mediated decarbonylation happens in

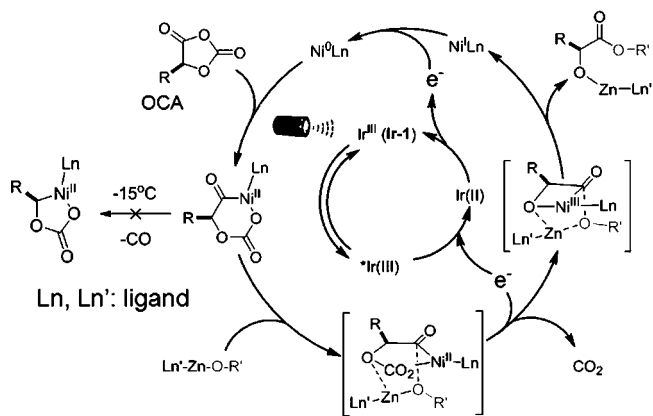


Figure 4. Proposed mechanism of controlled photoredox ring-opening polymerization of OCAs.

the photoredox decarbonylation reaction in an insignificant way;^{10b} however, such decarbonylation reaction considerably affects the photoredox ROP results especially for high DP polymers (Table 1, entry 2 versus 3; Figure 3). Given the wealth of reported Ni-catalyzed carbonylation and decarbonylation,^{22,25} the synergistic use of both low temperature and photoredox catalysts can be suggestive for other organic reactions.

CONCLUSIONS

In conclusion, the unprecedented Ni/Zn-mediated photoredox polymerization reported herein offers a strategy for achieving rapid, controlled OCA polymerization to prepare stereoregular PAHAs and PAHA copolymers bearing various functional side-chain groups. This strategy can be expected to enable the generation of PAHAs with desirable macroscopic properties such as rigidity, elasticity, and biodegradability and has the potential to allow for new fabrication techniques such as photolithography of biodegradable polyesters.²⁷

ASSOCIATED CONTENT

Supporting Information

The Supporting Information is available free of charge on the ACS Publications website at DOI: 10.1021/jacs.7b01462.

Materials, instruments and characterization, polymerization procedures, NMR spectra, additional tables and figures (PDF)

AUTHOR INFORMATION

Corresponding Author

*rtong@vt.edu

ORCID

Rong Tong: 0000-0002-2034-9272

Notes

The authors declare no competing financial interest.

ACKNOWLEDGMENTS

A provisional patent (U.S. Patent Application No.: 62/414,016) has been filed pertaining to the results presented in this paper. This work was supported by start-up funding from Virginia Polytechnic Institute and State University. We thank Dr. N. Murthy Shanaiah for NMR experiments and Dr. William Bebout for ESI-MS experiments.

REFERENCES

- (1) For selected reviews, see (a) Middleton, J. C.; Tipton, A. J. *Biomaterials* **2000**, *21*, 2335–2346. (b) Sudesh, K.; Abe, H.; Doi, Y. *Prog. Polym. Sci.* **2000**, *25*, 1503–1555. (c) Auras, R.; Harte, B.; Selke, S. *Macromol. Biosci.* **2004**, *4*, 835–864. (d) Zhu, Y.; Romain, C.; Williams, C. K. *Nature* **2016**, *540*, 354–362. (e) Hillmyer, M. A.; Tolman, W. B. *Acc. Chem. Res.* **2014**, *47*, 2390–2396.
- (2) (a) Albertsson, A. C.; Varma, I. K. *Biomacromolecules* **2003**, *4*, 1466–1486. (b) Vert, M. *Biomacromolecules* **2005**, *6*, 538–546. (c) van Krevelen, D. W.; Te Nijenhuis, K. *Properties of Polymers: Their Correlation with Chemical Structure; Their Numerical Estimation and Prediction from Additive Group Contributions*; Elsevier: Amsterdam, The Netherlands, 2009.
- (3) Recent review on lactide functionalization: Yu, Y.; Zou, J.; Cheng, C. *Polym. Chem.* **2014**, *5*, 5854–5872.
- (4) Representative examples of OCA synthesis and polymerization: (a) Thillaye du Boullay, O.; Marchal, E.; Martin-Vaca, B.; Cossio, F. P.; Bourissou, D. *J. Am. Chem. Soc.* **2006**, *128*, 16442–16443. (b) du Boullay, O. T.; Bonduelle, C.; Martin-Vaca, B.; Bourissou, D. *Chem. Commun.* **2008**, 1786–1788. (c) Pounder, R. J.; Fox, D. J.; Barker, I. A.;

- Bennison, M. J.; Dove, A. P. *Polym. Chem.* **2011**, *2*, 2204–2212. (d) Zhang, Z.; Yin, L.; Xu, Y.; Tong, R.; Lu, Y.; Ren, J.; Cheng, J. *Biomacromolecules* **2012**, *13*, 3456–3462. (e) Lu, Y.; Yin, L.; Zhang, Y.; Zhang, Z.; Xu, Y.; Tong, R.; Cheng, J. *ACS Macro Lett.* **2012**, *1*, 441–444. (f) Yin, Q.; Tong, R.; Xu, Y.; Baek, K.; Dobrucki, L. W.; Fan, T. M.; Cheng, J. *Biomacromolecules* **2013**, *14*, 920–929. (g) Chen, X.; Lai, H.; Xiao, C.; Tian, H.; Chen, X.; Tao, Y.; Wang, X. *Polym. Chem.* **2014**, *5*, 6495–6502.

(5) Recent reviews on OCA polymerization: (a) Martin Vaca, B.; Bourissou, D. *ACS Macro Lett.* **2015**, *4*, 792–798. (b) Yin, Q.; Yin, L.; Wang, H.; Cheng, J. *Acc. Chem. Res.* **2015**, *48*, 1777–1787.

(6) Buchard, A.; Carbery, D. R.; Davidson, M. G.; Ivanova, P. K.; Jeffery, B. J.; Kociok-Köhn, G. I.; Lowe, J. P. *Angew. Chem., Int. Ed.* **2014**, *53*, 13858–13861.

(7) Wang, R.; Zhang, J.; Yin, Q.; Xu, Y.; Cheng, J.; Tong, R. *Angew. Chem., Int. Ed.* **2016**, *55*, 13010–13014.

(8) Recent review on photoredox radical polymerization: Chen, M.; Zhong, M.; Johnson, J. A. *Chem. Rev.* **2016**, *116*, 10167–10211.

(9) Prier, C. K.; Rankic, D. A.; MacMillan, D. W. C. *Chem. Rev.* **2013**, *113*, 5322–5363.

(10) Representative examples of Ni-mediated photoredox reaction: (a) Zuo, Z. W.; Ahneman, D. T.; Chu, L. L.; Terrett, J. A.; Doyle, A. G.; MacMillan, D. W. C. *Science* **2014**, *345*, 437–440. (b) Le, C.; MacMillan, D. W. C. *J. Am. Chem. Soc.* **2015**, *137*, 11938–11941.

(11) (a) Deming, T. J. *Nature* **1997**, *390*, 386–389. (b) Deming, T. J. *J. Am. Chem. Soc.* **1998**, *120*, 4240–4241.

(12) (a) Cornella, J.; Edwards, J. T.; Qin, T.; Kawamura, S.; Wang, J.; Pan, C. M.; Gianatassio, R.; Schmidt, M.; Eastgate, M. D.; Baran, P. S. *J. Am. Chem. Soc.* **2016**, *138*, 2174–2177. (b) Qin, T.; Cornella, J.; Li, C.; Malins, L. R.; Edwards, J. T.; Kawamura, S.; Maxwell, B. D.; Eastgate, M. D.; Baran, P. S. *Science* **2016**, *352*, 801–805.

(13) Johnson, J. B.; Rovis, T. *Acc. Chem. Res.* **2008**, *41*, 327–338.

(14) Webster, O. W. *Science* **1991**, *251*, 887–893.

(15) Studer, A.; Curran, D. P. *Angew. Chem., Int. Ed.* **2016**, *55*, 58–102.

(16) Scott, N. M.; Clavier, H.; Mahjoor, P.; Stevens, E. D.; Nolan, S. P. *Organometallics* **2008**, *27*, 3181–3186.

(17) Williams, C. K.; Breyfogle, L. E.; Choi, S. K.; Nam, W.; Young, V. G., Jr.; Hillmyer, M. A.; Tolman, W. B. *J. Am. Chem. Soc.* **2003**, *125*, 11350–11359.

(18) Chamberlain, B. M.; Cheng, M.; Moore, D. R.; Ovitt, T. M.; Lobkovsky, E. B.; Coates, G. W. *J. Am. Chem. Soc.* **2001**, *123*, 3229–3238.

(19) Ouhadi, T.; Hamitou, A.; Jerome, R.; Teyssie, P. *Macromolecules* **1976**, *9*, 927–931.

(20) (a) Yeung, C. S.; Dong, V. M. *J. Am. Chem. Soc.* **2008**, *130*, 7826–7827. (b) Xiao, L.-J.; Fu, X.-N.; Zhou, M.-J.; Xie, J.-H.; Wang, L.-X.; Xu, X.-F.; Zhou, Q.-L. *J. Am. Chem. Soc.* **2016**, *138*, 2957–2960.

(21) Bodner, G. M. *Inorg. Chem.* **1975**, *14*, 1932–1935.

(22) (a) Ishizu, J.; Yamamoto, T.; Yamamoto, A. *Chem. Lett.* **1976**, *5*, 1091–1094. (b) Yamamoto, T.; Igarashi, K.; Ishizu, J.; Yamamoto, A. *J. Chem. Soc., Chem. Commun.* **1979**, 554–555. (c) Yamamoto, T.; Ishizu, J.; Yamamoto, A. *J. Am. Chem. Soc.* **1981**, *103*, 6863–6869. (d) Yamamoto, T.; Sano, K.; Yamamoto, A. *J. Am. Chem. Soc.* **1987**, *109*, 1092–1100.

(23) Jiang, L.; Xu, Q. *J. Am. Chem. Soc.* **2005**, *127*, 8906–8907.

(24) Dunbar, K. R.; Haefner, S. C. *Inorg. Chem.* **1992**, *31*, 3676–3679.

(25) For examples, see (a) Kajita, Y.; Kurahashi, T.; Matsubara, S. *J. Am. Chem. Soc.* **2008**, *130*, 17226–17227. (b) Kajita, Y.; Matsubara, S.; Kurahashi, T. *J. Am. Chem. Soc.* **2008**, *130*, 6058–6059. (c) Yoshino, Y.; Kurahashi, T.; Matsubara, S. *J. Am. Chem. Soc.* **2009**, *131*, 7494–7495.

(26) Johnson, J. B.; Bercot, E. A.; Rowley, J. M.; Coates, G. W.; Rovis, T. *J. Am. Chem. Soc.* **2007**, *129*, 2718–2725.

(27) (a) Hawker, C. J.; Russell, T. P. *MRS Bull.* **2005**, *30*, 952–966. (b) Tumbleston, J. R.; Shirvanyants, D.; Ermoshkin, N.; Januszewicz, R.; Johnson, A. R.; Kelly, D.; Chen, K.; Pinschmidt, R.; Rolland, J. P.; Ermoshkin, A.; Samulski, E. T.; DeSimone, J. M. *Science* **2015**, *347*, 1349–1352.